

Excited-State Dynamics of Structurally Characterized $[\text{Re}^{\text{I}}(\text{CO})_3(\text{phen})(\text{HisX})]^+$ ($X = 83, 109$) *Pseudomonas aeruginosa* Azurins in Aqueous Solution

Ana María Blanco-Rodríguez,[†] Michael Busby,[†] Cristian Grădinaru,[‡]
 Brian R. Crane,^{*,‡} Angel J. Di Bilio,[§] Pavel Matousek,^{||} Michael Towrie,^{||}
 Brian S. Leigh,[⊥] John H. Richards,[§] Antonín Vlček, Jr.,^{*,†} and Harry B. Gray^{*,⊥}

Contribution from the School of Biological and Chemical Sciences, Queen Mary, University of London, Mile End Road, London E1 4NS, United Kingdom, Department of Chemistry and Chemical Biology, Cornell University, Ithaca, New York 14853, Division of Chemistry and Chemical Engineering, California Institute of Technology, Pasadena, California 91125, Central Laser Facility, CCLRC Rutherford Appleton Laboratory, Chilton, Didcot, Oxfordshire OX11 0QX, United Kingdom, and Beckman Institute, California Institute of Technology, Pasadena, California 91125

Received November 1, 2005; E-mail: crane@bonobo.chem.cornell.edu; a.vlcek@qmul.ac.uk; hbgray@caltech.edu

Abstract: The triplet metal-to-ligand charge transfer (³MLCT) dynamics of two structurally characterized $\text{Re}^{\text{I}}(\text{CO})_3(\text{phen})(\text{HisX})$ -modified (phen = 1,10-phenanthroline; X = 83, 109) *Pseudomonas aeruginosa* azurins have been investigated by picosecond time-resolved infrared (TRIR) spectroscopy in aqueous (D_2O) solution. The ³MLCT relaxation dynamics exhibited by the two Re^{I} -azurins are very different from those of the sensitizer $[\text{Re}^{\text{I}}(\text{CO})_3(\text{phen})(\text{im})]^+$ (im = imidazole). Whereas the $\text{Re}^{\text{I}}(\text{CO})_3$ intramolecular vibrational relaxation in $\text{Re}^{\text{I}}(\text{CO})_3(\text{phen})(\text{HisX})\text{Az}$ (4 ps) is similar to that of $[\text{Re}^{\text{I}}(\text{CO})_3(\text{phen})(\text{im})]^+$ (2 ps), the medium relaxation is much slower (~250 vs 9.5 ps); the 250-ps relaxation is attributable to reorientation of D_2O molecules as well as structural reorganization of the rhenium chromophore and nearby polar amino acids in each of the modified proteins.

Introduction

Much of our current understanding of biological electron transfer (ET) is based on investigations of structurally characterized Re^{I} - and Ru^{II} -diimine derivatives of *Pseudomonas aeruginosa* azurin.^{1–8} Activationless $\text{Cu}^{\text{I}} \rightarrow \text{Ru}^{\text{III}}$ ET rates in $\text{Ru}(\text{HisX})$ -azurins ($X = 83, 122, 124, 126, 107, 109$) have established a timetable for distant electron tunneling through proteins. Although not a factor in activationless or inverted ET reactions, either solvent or polypeptide conformational dynamics

could become rate-limiting at lower driving forces;^{6,7} and water dynamics near protein surfaces is of special interest, as structured water and water-mediated hydrogen bonds at protein–protein interfaces are believed to enhance the couplings between distant redox centers.^{9–12}

We have initiated an experimental program with the goal of determining time scales for polypeptide and solvent dynamics in metal-labeled proteins: $[\text{Re}^{\text{I}}(\text{CO})_3(\text{phen})(\text{His})]^+$ (phen = 1,10-phenanthroline) complexes have been selected for initial study, as the $\text{C}\equiv\text{O}$ stretching vibrational dynamics of electronically excited Re^{I} carbonyls^{13–25} are very sensitive to conformational flexibility as well as the degree of hydration in the region near

[†] University of London.

[‡] Cornell University.

[§] Division of Chemistry and Chemical Engineering, California Institute of Technology.

^{||} CCLRC Rutherford Appleton Laboratory.

[⊥] Beckman Institute, California Institute of Technology.

- (1) Winkler, J. R.; Di Bilio, A. J.; Farrow, N. A.; Richards, J. H.; Gray, H. B. *Pure Appl. Chem.* **1999**, *71*, 1753–1764.
- (2) Di Bilio, A. J.; Crane, B. R.; Wehbi, W. A.; Kiser, C. N.; Abu-Omar, M. M.; Carlos, R. M.; Richards, J. H.; Winkler, J. R.; Gray, H. B. *J. Am. Chem. Soc.* **2001**, *123*, 3181–3182.
- (3) Crane, B. R.; Di Bilio, A. J.; Winkler, J. R.; Gray, H. B. *J. Am. Chem. Soc.* **2001**, *123*, 11623–11631.
- (4) Miller, J. E.; Di Bilio, A. J.; Wehbi, W. A.; Green, M. T.; Museth, A. K.; Richards, J. R.; Winkler, J. R.; Gray, H. B. *Biochim. Biophys. Acta: Bioenergetics* **2004**, *1655*, 59–63.
- (5) Museth, A. K.; Abrahamsson, M. L. A.; Miller, J. E.; Grădinaru, C.; Crane, B. R.; Di Bilio, A. J.; Leigh, B. S.; Richards, J. H.; Winkler, J. R.; Gray, H. B., in preparation.
- (6) Gray, H. B.; Winkler, J. R. *Q. Rev. Biophys.* **2003**, *36*, 341–372.
- (7) Gray, H. B.; Winkler, J. R. *Proc. Natl. Acad. Sci. U.S.A.* **2005**, *102*, 3534–3539.
- (8) Skourtis, S. S.; Balabin, I. A.; Kawatsu, T.; Beratan, D. N. *Proc. Natl. Acad. Sci. U.S.A.* **2005**, *102*, 3552–3557.

- (9) Lin, J. P.; Balabin, I. A.; Beratan, D. N. *Science* **2005**, *310*, 1311–1313.
- (10) Tezcan, F. A.; Crane, B. R.; Winkler, J. R.; Gray, H. B. *Proc. Natl. Acad. Sci. U.S.A.* **2001**, *98*, 5002–5006.
- (11) Francisco, W. A.; Wille, G.; Smith, A. J.; Merkle, D. J.; Klinman, J. P. *J. Am. Chem. Soc.* **2004**, *126*, 13168–13169.
- (12) Miyashita, O.; Okamura, M. Y.; Onuchic, J. N. *Proc. Natl. Acad. Sci. U.S.A.* **2005**, *102*, 3558–3563.
- (13) George, M. W.; Johnson, F. P. A.; Westwell, J. R.; Hodges, P. M.; Turner, J. J. *J. Chem. Soc., Dalton Trans.* **1993**, 2977–2979.
- (14) Gamelin, D. R.; George, M. W.; Glyn, P.; Grevels, F. W.; Johnson, F. P. A.; Klotzbucher, W.; Morrison, S. L.; Russell, G.; Schaffner, K.; Turner, J. J. *Inorg. Chem.* **1994**, *33*, 3246–3250.
- (15) Stor, G. J.; Hartl, F.; van Outersterp, J. W. M.; Stufkens, D. J. *Organometallics* **1995**, *14*, 1115–1131.
- (16) Clark, I. P.; George, M. W.; Johnson, F. P. A.; Turner, J. J. *Chem. Commun.* **1996**, 1587–1588.
- (17) Bignozzi, C. A.; Schoonover, J. R.; Dyer, R. B. *Comments Inorg. Chem.* **1996**, *18*, 77–100.
- (18) Schoonover, J. R.; Strouse, G. F.; Omberg, K. M.; Dyer, R. B. *Comments Inorg. Chem.* **1996**, *18*, 165–188.
- (19) Schoonover, J. R.; Strouse, G. F. *Chem. Rev.* **1998**, *98*, 1335–1355.

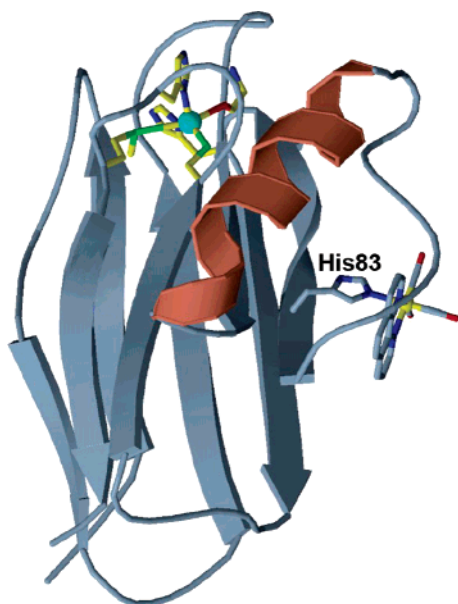


Figure 1. Structure of $\text{Re}^{\text{I}}(\text{CO})_3(\text{phen})(\text{His83})\text{Az}$ (PDB code 1JZI).³ Azurin is a well-characterized blue-copper protein^{3,27,28} whose active center is embedded in an 8-stranded antiparallel β barrel, with one extra-barrel helix in the 128-residue chain inserted between β_4 and β_5 (numbered from the N-terminus). The copper ion is trigonally coordinated by donor atoms from the side chains of Cys112, His46, and His117 in a hydrophobic cluster at one end of the β barrel; and the Met121 thioether and Gly45 peptide carbonyl are weak axial ligands.^{3,29,30} In the $\text{Re}^{\text{I}}(\text{CO})_3(\text{phen})(\text{His83})$ protein, the sensitizer produces only minor changes in the structure of the folded polypeptide. His83 is replaced by Gln in (His109)Az.

the metallolabel. Both the native and the His109-mutant proteins react with $[\text{Re}^{\text{I}}(\text{CO})_3(\text{phen})(\text{H}_2\text{O})]^+$ to give $\text{Re}^{\text{I}}(\text{CO})_3(\text{phen})(\text{HisX})\text{Az}$ ($X = 83, 109$) derivatives.^{2,26} Here, we report the crystal structure of $\text{Re}^{\text{I}}(\text{CO})_3(\text{phen})(\text{His109})\text{Az}$ as well as details of the outer-sphere environment of the rhenium unit in the structure of $\text{Re}^{\text{I}}(\text{CO})_3(\text{phen})(\text{His83})\text{Az}$ determined previously (Figure 1).^{2,3} The excited-state dynamics of these structurally characterized Re^{I} -azurins and $[\text{Re}^{\text{I}}(\text{CO})_3(\text{phen})(\text{im})]^+$ ($\text{im} = \text{imidazole}$) in aqueous (D_2O) solution have been elucidated by picosecond time-resolved infrared (TRIR) spectroscopy.

Experimental Section

$\text{Re}^{\text{I}}(\text{CO})_3(\text{phen})(\text{HisX})\text{Az}$ ($X = 83, 109$) derivatives were prepared by reacting protein with 5 mM *fac*- $[\text{Re}^{\text{I}}(\text{CO})_3(\text{phen})(\text{H}_2\text{O})]\text{CF}_3\text{SO}_3$.^{2,26} (His109)Az was incubated with the Re^{I} -aquo complex for 3 weeks or longer at 37 °C. Solutions for TRIR were prepared by repeatedly concentrating and diluting protein with KPi buffer using Centricon devices. The buffer was prepared by dissolving $\text{K}_2\text{HPO}_4 \cdot 3\text{H}_2\text{O}$ up to 26.8 mM and KH_2PO_4 up to 19.8 mM in D_2O ($\mu \approx 100$ mM). The uncorrected pD at 21 °C of the buffer solution was 7.1. Reduced (Cu^{I}) Re^{I} -azurin was made by addition of sodium dithionite in D_2O until the blue color disappeared.

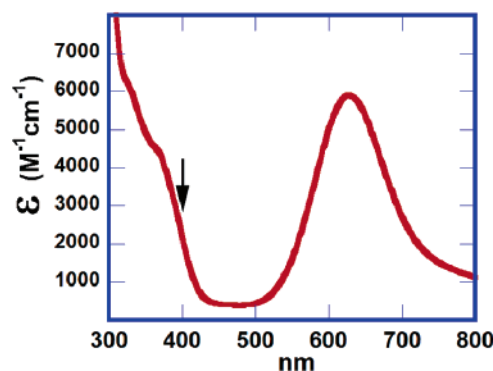
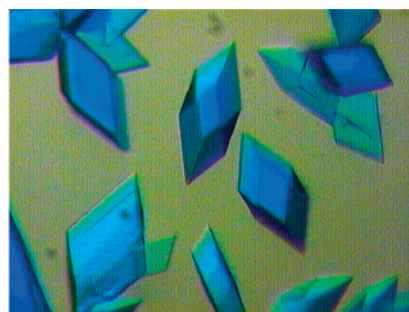


Figure 2. Crystals of $\text{Re}^{\text{I}}(\text{CO})_3(\text{phen})(109\text{His})\text{AzCu}(\text{II})$ (upper panel) and UV-visible absorption spectrum of an aqueous solution (H_2O) of the same protein (lower panel). The arrow in the lower panel marks the TRIR excitation wavelength.

Crystals of $[\text{Re}^{\text{I}}(\text{CO})_3(\text{phen})-(\text{Met}109\text{His})]^+(\text{His}83\text{Gln})\text{AzCu}(\text{II})$ (space group $P1$, cell dimensions $30.935 \times 38.334 \times 48.835 \text{ \AA}$; $\alpha = 100.50^\circ$, $\beta = 106.25^\circ$, $\gamma = 109.43^\circ$, two molecules per asymmetric unit) grew from 2 μL drops made from equal volumes of 30 mg/mL Re^{I} -azurin in 25 mM HEPES pH 7.5 and reservoir containing 20% PEG molecular weight 4000, 100 mM LiNO_3 , and 100 mM imidazole pH 7.0. Diffraction data (30.0–1.4 Å resolution, 80.7% complete, $R_{\text{sym}} = \sum_j |I_j - \langle I \rangle| / \sum_j I_j = 6.6\%$; overall signal-to-noise = $\langle I \rangle / \sigma I = 17.5$) were collected on a Quantum-210 CCD (Area Detector Systems Corp.), at the Cornell High Energy Synchrotron Source, beamline F2 (0.945 Å), and processed with DENZO.³¹ The structure of $\text{Re}^{\text{I}}(\text{CO})_3(\text{phen})-(\text{His}109)\text{AzCu}(\text{II})$ was determined by molecular replacement with EPMR³² using a probe derived from the structure of $\text{Ru}^{\text{II}}(2,2'$ -bipyridine)₂(im)(His83)AzCu(II) (PDB code 1BEX).³³ Rigid-body, positional, and thermal factor refinement with CNS,³⁴ amidst rounds of manual rebuilding, $\text{Re}^{\text{I}}(\text{CO})_3(\text{phen})$ incorporation, and water placement with XFIT,³⁵ followed by further anisotropic refinement of all heavy atoms' temperature factors (S, Cu, and Re) with SHELX-97³⁶ produced the final model (1.4 Å resolution, R -factor (all observed reflections) = 19.5%; R -free = 22.7%). The refinement was performed

- (20) Asbury, J. B.; Wang, Y.; Lian, T. Q. *Bull. Chem. Soc. Jpn.* **2002**, *75*, 973–983.
 (21) Dattelbaum, D. M.; Meyer, T. J. *J. Phys. Chem. A* **2002**, *106*, 4519–4524.
 (22) Dattelbaum, D. M.; Omberg, K. M.; Schoonover, J. R.; Martin, R. L.; Meyer, T. J. *Inorg. Chem.* **2002**, *41*, 6071–6079.
 (23) Dattelbaum, D. M.; Omberg, K. M.; Hay, P. J.; Gebhart, N. L.; Martin, R. L.; Schoonover, J. R.; Meyer, T. J. *J. Phys. Chem. A* **2004**, *108*, 3527–3536.
 (24) Dattelbaum, D. M.; Martin, R. L.; Schoonover, J. R.; Meyer, T. J. *J. Phys. Chem. A* **2004**, *108*, 3518–3526.
 (25) Liard, D. J.; Busby, M.; Matousek, P.; Towrie, M.; Vlček, A., Jr. *J. Phys. Chem. A* **2004**, *108*, 2363–2369.
 (26) Connick, W. B.; Di Bilio, A. J.; Schaefer, W. P.; Gray, H. B. *Acta Crystallogr.* **1999**, *C55*, 913–916.

- (27) Adman, E. T. *Adv. Protein Chem.* **1991**, *42*, 145–197.
 (28) Gray, H. B.; Malmström, B. G.; Williams, R. J. P. *J. Biol. Inorg. Chem.* **2000**, *5*, 551–559.
 (29) Shepard, W. E. B.; Anderson, B. F.; Lewandoski, D. A.; Norris, G. E.; Baker, E. N. *J. Am. Chem. Soc.* **1990**, *112*, 7817–1719.
 (30) Nar, H.; Messerschmidt, A.; Huber, R.; van de Kamp, M.; Canters, G. W. *J. Mol. Biol.* **1991**, *221*, 765–772.
 (31) Otwinowski, Z.; Minor, M. *Methods Enzymol.* **1997**, *276*, 307–326.
 (32) Kissinger, C. R.; Gehlhaar, D. K.; Fogel, D. B. *Acta Crystallogr.* **1999**, *D55*, 484–491.
 (33) Faham, S.; Day, M. W.; Connick, W. B.; Crane, B. R.; Di Bilio, A. J.; Schaefer, W. P.; Rees, D. C.; Gray, H. B. *Acta Crystallogr.* **1999**, *D55*, 379–385.
 (34) Brunger, A.; Adams, P. D.; Clore, G. M.; DeLano, W. L.; Gros, P.; Grosse-Kunstleve, R. W.; Jiang, J. S.; Kuszewski, J.; Nilges, M.; Pannu, N. S.; Read, R. J.; Rice, L. M.; Simonson, T.; Warren, G. L. *Acta Crystallogr.* **1998**, *D54*, 905–921.
 (35) McRee, D. E. *J. Mol. Graphics* **1992**, *10*, 44–46.
 (36) Sheldrick, G. M.; Schneider, T. R. SHELXL: High-resolution refinement. In *Macromolecular Crystallography, Pt. B*; 1997; Vol. 277, pp 319–343.

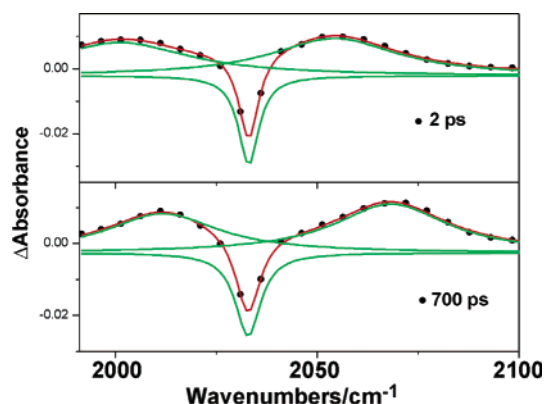


Figure 3. TRIR spectra of Re^I(CO)₃(phen)(His109)AzCu(II) measured at 2 (upper panel) and 700 ps (lower panel). The spectra at each time delay were fitted with Lorentzian functions. Black, experimental points; green, individual Lorentzian peaks; red, simulated TRIR spectrum.

against all but 5% of the reflections, which were used to calculate an *R*-free value. The final round of refinement was performed against the entire dataset. All residues have favored backbone dihedral angles. Stereochemical restraints were removed from the copper ligand bonds in the later stages of refinement.

The TRIR measurements were conducted using equipment and procedures described previously.^{37–39} Samples were excited at 400 nm (~3 μJ energy) using frequency-doubled 150-fs pulses from a Ti:sapphire laser. The excitation beam was focused on an area of ~200 μm. IR-probe pulses (~150 fs) obtained by difference-frequency generation covered a spectral range of 150–200 cm⁻¹. Samples were placed in a 0.5–0.1 mm CaF₂ IR cell, which was rastering in two dimensions.

The TRIR measurements on the Re^I-modified proteins were complicated by the necessity to use an aqueous solvent and a relatively low concentration (~5 mM) of rhenium chromophore. Thus, the transient IR signals were weak (ΔOD < 0.05) and measured against a relatively large background. However, reliable spectra were measured by using D₂O as solvent (some H₂O is inevitably present, however), short optical path lengths (≤0.1 mm), and mechanical rastering of the IR cell to prevent local overheating of the sample. The spectra were fitted with Lorentzian functions to determine accurately their band positions and shapes. Fits were conducted on the middle excited-state band, the A'(1) bleach, and the A'(1) excited-state band (limiting the fittings to the latter three bands allowed a more accurate determination of the position of the A'(1) excited-state band). Typical fits are shown in Figure 3. Spectral and kinetics fitting procedures were conducted using MicroCal Origin 7.0.

Results

The crystal structures of the two Re^I-azurins (Figures 4 and 5) reveal that the rhenium complex does not significantly perturb the protein fold. In particular, the geometry of the copper site is identical to that of unmodified azurin.³³ Of particular interest is the observation of two orientations (70–75% and 25–30%) of the rhenium complex in crystals of Re^I(CO)₃(phen)-(His109)AzCu(II) (Figure 5).

The ground-state ν(CO) IR spectra of Re^I(CO)₃(phen)(His83)-Az and Re^I(CO)₃(phen)(His109)Az exhibit a sharp band at

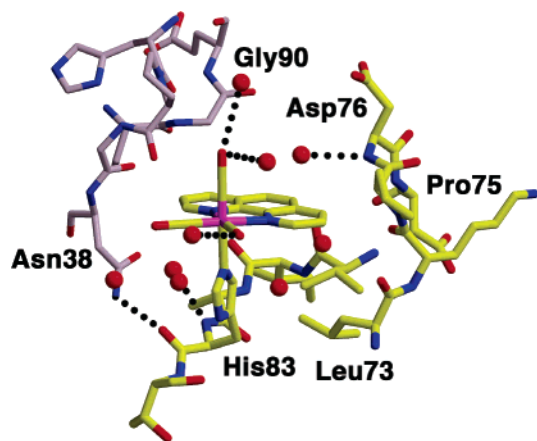


Figure 4. Structure of Re^I(CO)₃(phen)(His83)Az (PDB code 1JZI) in the region of the rhenium complex. The environment surrounding the rhenium complex is significantly different from that expected for [Re^I(CO)₃(phen)-(im)]⁺ in aqueous solution. The rhenium complex buries 170 Å² of accessible surface area on the azurin molecule to which it is bound, and about 40% of the accessible surface area of the rhenium complex is buried by the protein. In addition to this primary interaction, an adjacent molecule in the crystal lattice (gray bonds) further sequesters the rhenium complex. The Re^I(CO)₃(phen) unit is covalently bound to His83 N^{δ2} and packs against an otherwise surface-exposed loop between the lone α-helix and a fifth β-strand of the azurin β-barrel. The imidazole ring of His83 hydrogen bonds with the carbonyl O atom of Thr48 [His83 N^{δ1}...Thr48 O] (not shown) and occupies the same position as found in native azurin. In addition to covalent attachment to His83, interactions of the rhenium complex with the protein are dominated by packing of the phen ligand against Val80 and Ile81 in the center of the β-α loop and the close proximity of four negatively charged residues to the label: Asp71, Asp76, Asp77, and Asp93. Residues Leu73, Lys74, Asp76, Asp77, Val80, Ile81, and His83 all contact the phen ligand directly. With the exception of a slight change in the conformation in Asp76, whose C_α moves 1.28 Å to accommodate the rhenium complex, the structure of the folded polypeptide is virtually the same as that of native azurin (PDB code 4AZU).

~2030 cm⁻¹ and a broad band at ~1925 cm⁻¹, which correspond to A'(1) and (nearly) degenerate A'(2) + A'' CO stretching vibrations, respectively (Figure 6). In the case of Re^I(CO)₃(phen)(His109)Az, the lower band is split into two components. The ground-state CO stretching frequencies are set out in Table 1.

Laser excitation (400-nm pulses, ~150 fs) in the onset region of the MLCT absorption band of the rhenium chromophore (Figure 2, lower panel) partially depletes the ground-state population, as manifested by the appearance of negative (bleach) and positive transient bands in the difference TRIR spectra (Figure 7). All of these features are formed within the instrument time resolution. The excited-state ν(CO) bands shift to higher wavenumbers and narrow with increasing time delay from excitation. This dynamic evolution is most prominent for the middle and the highest bands that are attributed²⁴ to the out-of-phase A'(2) and in-phase A'(1) symmetrical CO vibrations, respectively. The ν(CO) values of the relaxed excited states (determined at long time delays) are given in Table 1.

The dynamics of the upward shift was analyzed by monitoring the time dependences of the A'(1) band positions ν(*t*) (in cm⁻¹), which were found to follow biexponential kinetics (Figure 8, eq 1):

$$\nu(t) = \nu(\infty) - A_f \exp(-t/\tau_f) - A_s \exp(-t/\tau_s) \quad (1)$$

In eq 1, ν(∞) is the final band position extrapolated to infinite time delay, τ_f and τ_s are the time constants of the fast and slow

- (37) Towrie, M.; Grills, D. C.; Dyer, J.; Weinstein, J. A.; Matousek, P.; Barton, R.; Bailey, P. D.; Subramaniam, N.; Kwok, W. M.; Ma, C. S.; Phillips, D.; Parker, A. W.; George, M. W. *Appl. Spectrosc.* **2003**, *57*, 367–380.
 (38) Vlček, A., Jr.; Farrell, I. R.; Liard, D. J.; Matousek, P.; Towrie, M.; Parker, A. W.; Grills, D. C.; George, M. W. *J. Chem. Soc., Dalton Trans.* **2002**, 701–712.
 (39) Busby, M.; Gabrielsson, A.; Matousek, P.; Towrie, M.; Di Bilio, A. J.; Gray, H. B.; Vlček, A., Jr. *Inorg. Chem.* **2004**, *43*, 4994–5002.

Table 1. Ground- and Excited-State CO Stretching Frequencies (cm^{-1})^a

compound	ground state			excited state			$\Delta\nu(A'(1))$	$\Delta\nu \text{ Av.}$
	A''	A'(2)	A'(1)	A'' ^b	A'(2) ^b	A'(1) ^c		
$[\text{Re}^{\text{I}}(\text{CO})_3(\text{phen})(\text{im})]^+$	1925	1925	2032	1968	2013	2071	+39	+57
$\text{Re}^{\text{I}}(\text{CO})_3(\text{phen})(\text{His83})\text{Az}$	1923	1923	2031	1967	2011	2068	+37	+56
$\text{Re}^{\text{I}}(\text{CO})_3(\text{phen})(\text{His109})\text{Az}$	1918	1932	2032	1966	2010	2067	+35	+54

^a For band assignments, see ref 24. ^b Frequencies measured at long time delays (1 ns). ^c Frequencies extrapolated to infinite time delay ($\nu(\infty)$).

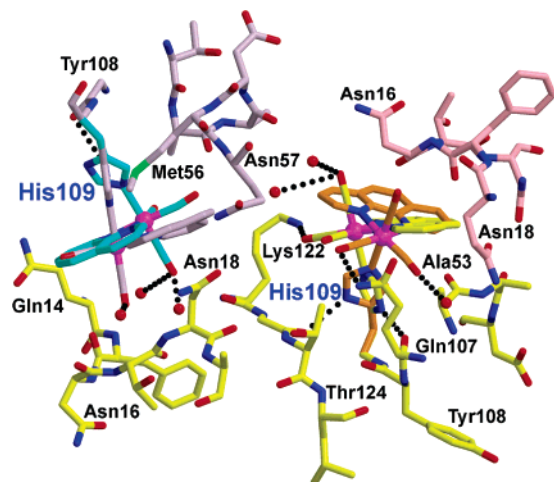


Figure 5. Structure of $\text{Re}^{\text{I}}(\text{CO})_3(\text{phen})(\text{His109})\text{Az}$ (PDB code 2FNW) in the region of the rhenium complex. Two Re^{I} -azurin molecules per asymmetric unit generate different environments for the two rhenium complexes in the crystal lattice (three different azurin molecules are shown with yellow, gray, and pink bonds). Both rhenium complexes mediate contacts between neighboring molecules and bury $\sim 155 \text{ \AA}^2$ of solvent-accessible surface on the covalently attached azurin molecule. Conversely, about 40% of the rhenium complex surface area is buried by the protein in each case. The $\text{Re}^{\text{I}}(\text{CO})_3(\text{phen})$ unit is covalently attached to His109 $\text{N}^{\text{e}2}$ and packs against an otherwise surface-exposed loop between the first and second β -strand of the azurin β -barrel. Both unique azurin molecules show two distinct conformations for the rhenium complex (yellow and orange; gray and cyan). In one of the two conformers (orange and gray), His109 is hydrogen-bonded to the carbonyl oxygen of Gly123 [$\text{His109 N}^{\text{d}1} \cdots \text{Gly123 O}$]. In the other conformer (yellow and cyan), the imidazole ring of His109 forms a hydrogen bond with the carbonyl O atom of Tyr108 [$\text{His109 N}^{\text{d}1} \cdots \text{Tyr108 O}$]. In one molecule, the N^{c} of Lys122 forms a hydrogen bond with an equatorial carbonyl ligand [$\text{Lys122 N}^{\text{c}} \cdots \text{OC-Re}^{\text{I}}$]. The rhenium complex directly contacts the main chain of Asn16 and Thr17 and the side chains of Asn18 and Gln14. Little, if any, conformational change is observed in the folding of the loops contacting the rhenium complex in either molecule.

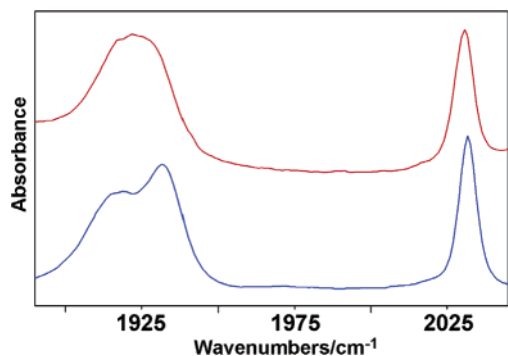


Figure 6. FTIR absorption spectra of $\text{Re}^{\text{I}}(\text{CO})_3(\text{phen})(\text{His83})\text{AzCu}(\text{II})$ (red trace) and $\text{Re}^{\text{I}}(\text{CO})_3(\text{phen})(\text{His109})\text{AzCu}(\text{II})$ (blue trace).

components of the shift, and A_f and A_s are the corresponding amplitudes. The magnitude of the total shift upon excitation is defined as $\nu(\infty) - \nu(\text{GS})$, while $A_f + A_s$ is the magnitude of the dynamic shift and $\nu(\text{GS})$ is the band position in the ground

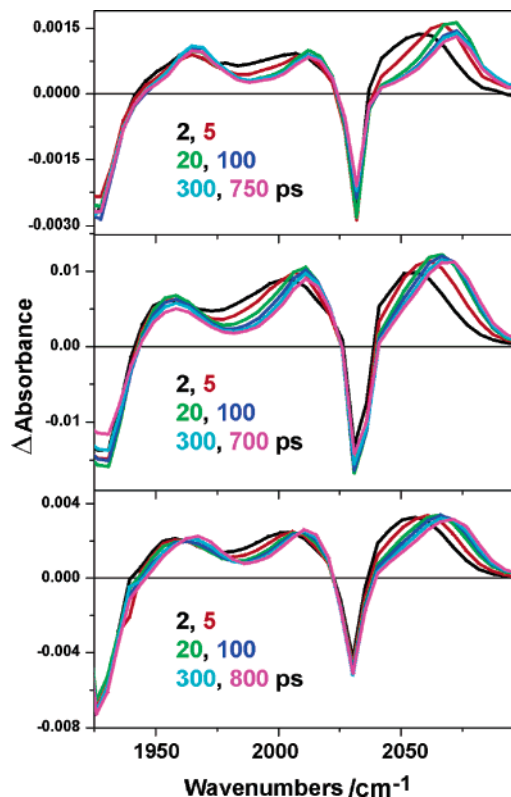


Figure 7. Difference TRIR spectra of $[\text{Re}^{\text{I}}(\text{CO})_3(\text{phen})(\text{im})]^+$ (upper panel), $\text{Re}^{\text{I}}(\text{CO})_3(\text{phen})(\text{His83})\text{AzCu}(\text{II})$ (middle panel), and $\text{Re}^{\text{I}}(\text{CO})_3(\text{phen})(\text{His109})\text{AzCu}(\text{II})$ (lower panel) at various time delays. Separation between experimental points is $4\text{--}5 \text{ cm}^{-1}$.

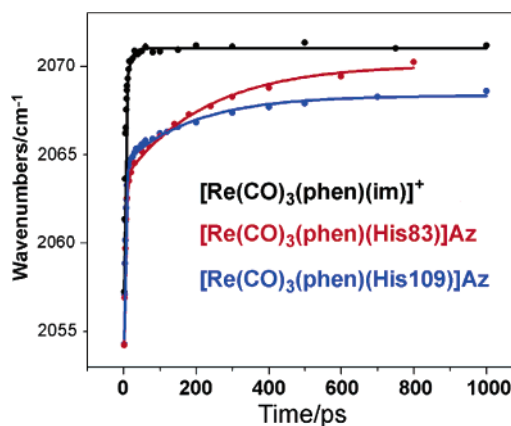


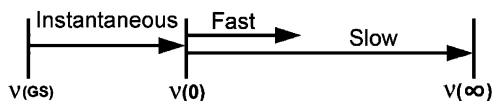
Figure 8. Biexponential fits (solid lines) of the time dependences of the positions of excited-state $A'(1) \nu(\text{CO})$ bands of $\text{Re}^{\text{I}}(\text{CO})_3(\text{phen})(\text{His}X)\text{Az}$ ($X = 83, 109$) and $[\text{Re}^{\text{I}}(\text{CO})_3(\text{phen})(\text{im})]^+$ (see Table 2).

state. As the total shift is larger than the dynamic shift, it follows that part of the shift is instantaneous, complete within the instrument time resolution. Its magnitude can be estimated as $\nu(0) - \nu(\text{GS})$, where $\nu(0)$ is the peak position extrapolated to time zero; $\nu(0) = \nu(\infty) - (A_f + A_s)$. The band-shift parameters,

Table 2. Dynamic Shift Parameters for the A'(1) $\nu(\text{CO})$ Band of Re^I–Azurins and [Re^I(CO)₃(phen)(im)]⁺

	Re ^I (CO) ₃ -(phen)(His83)Az	Re ^I (CO) ₃ -(phen)(His109)Az	[Re ^I (CO) ₃ -(phen)(im)] ⁺
$\nu(\text{GS}), \text{cm}^{-1}$	2030.5	2032	2032
$\nu_{\text{ES}}(\infty), \text{cm}^{-1}$	2068.1	2066.9	2071
total shift ^a	38	35	39
inst. shift ^b	18	14	9
dyn. shift	20	21	30
A_s, cm^{-1}	5.4 ± 0.3	4.1 ± 0.2	5.3 ± 1.4
A_f, cm^{-1}	14.3 ± 0.6	16.5 ± 0.5	24.9 ± 1.4
τ_s, ps	267 ± 44	227 ± 32	9.5 ± 2
τ_f, ps	4.3 ± 0.3	3.9 ± 0.2	2.1 ± 0.2
A_s/A_f	0.38	0.25	0.21
% A_s	27	20	18

^a $\nu_{\text{ES}}(\infty) - \nu(\text{GS})$, in cm^{-1} . ^b $\nu_{\text{ES}}(0) - \nu(\text{GS}) = \nu_{\text{ES}}(\infty) - A_f - A_s - \nu(\text{GS})$, in cm^{-1} . ^c $A_f + A_s$, in cm^{-1} . ^d $100A_s/(A_s + A_f)$.

Scheme 1. Dynamic Behavior of the Position of the A'(1) $\nu(\text{CO})$ Band after Excitation^a

^a The $\nu(\text{CO})$ band undergoes an “instantaneous” shift upon excitation from the ground-state position $\nu(\text{GS})$ to $\nu(0)$, which is followed by a dynamic shift to the final position $\nu(\infty)$. The dynamic shift occurs with two kinetics components, denoted “slow” and “fast”; see eq 1.

determined by biexponential fits of experimental $\nu(t)$, are set out in Table 2, and the observed dynamics is qualitatively depicted in Scheme 1.

The effect of reduction of the Cu^{II} center was determined for Re^I(CO)₃(phen)(His83)Az. Neither the positions nor the intensities of the ground-state IR bands nor their behavior after excitation were affected by reduction of the copper with sodium dithionite.

Discussion

The ground-state FTIR spectra of Re^I(CO)₃(phen)(His83)Az and [Re^I(CO)₃(phen)(im)]⁺ in the region of CO stretching vibrations are typical of [Re^I(CO)₃(N,N)(N-donor)]⁺ complexes.^{22–25,39} Characteristically, the A'(2) and A'' vibrations merge into a single band. In contrast, these vibrations are separated by 14 cm^{-1} in the case of Re^I(CO)₃(phen)(His109)Az. In crystals of Re^I(CO)₃(phen)(His109)Az, one of the equatorial COs is H-bonded to the N^δ of Lys122 in 50% of the molecules of one conformer (Figure 5); thus, for that conformer, the two equatorial CO's are coupled very differently to the outer-sphere region, as the 14- cm^{-1} splitting indicates. As the rotational barrier of the rhenium complex bound to His109 is likely low, we expect that several conformations of the rhenium unit in Re^I(CO)₃(phen)(His109)Az are populated in solution.

Excited-State Character. The TRIR data clearly show that the lowest excited state of [Re^I(CO)₃(phen)(im)]⁺ is ³MLCT, as demonstrated by the shift of the $\nu(\text{CO})$ spectral pattern to higher wavenumbers and splitting of the lower $\nu(\text{CO})$ band into two components upon excitation (Figure 7).^{13,14,16–25,39–41} The spectral shift is caused by depopulation of the $d\pi$ orbitals of the Re^I(CO)₃ core and strengthening of OC → Re σ donation,²² whereas the splitting of the lower band into distinct A'' and

A'(2) components reflects a change of the Re^I(CO)₃ local symmetry from pseudo- C_{3v} to C_s upon reduction of the phen ligand in the MLCT excited state. Small quantitative differences aside, the $\nu(\text{CO})$ IR absorption patterns of the relaxed excited state of both Re^I–azurins are the same as that seen for [Re^I(CO)₃(phen)(im)]⁺, thereby confirming that the electronic structure of the ³MLCT excited state does not change upon binding to the protein. This conclusion is in agreement with emission data.⁴²

The total A'(1) band shift upon excitation reflects the change of electron-density distribution in the chromophore between the relaxed excited state and the ground state. The A'(1) band shift has a similar magnitude for the Re^I–azurins and [Re^I(CO)₃(phen)(im)]⁺ (35–39 cm^{-1}). We conclude that the charge redistribution in the Re^I(CO)₃(phen)(im) chromophore in the thermally equilibrated (i.e., relaxed) excited state is about the same in bulk D₂O or bound to protein.

As discussed above, the A'(1) band-shift can be divided into instantaneous and dynamic parts, the latter occurring with “fast” and “slow” kinetics components (Scheme 1). The kinetics of the A'(1) band shift was analyzed using eq 1.⁴³ Inspection of Table 2 and Figure 8 shows that the excited-state dynamics of Re^I–azurins is very different from that of [Re^I(CO)₃(phen)(im)]⁺. The slow kinetics component of the dynamic shift is much slower for the Re^I–azurins. This behavior can be explained as a medium response to the change of the magnitude and direction of the dipole moment of the Re^I(CO)₃(phen) chromophore upon excitation to the Re^{II}(CO)₃(phen^{•-}) ³MLCT state. Initially, the polar environment would be arranged to optimize electrostatic interactions with the ground-state chromophore. Upon excitation, only nearby molecules would respond immediately; reorientation of the outer environment would be much slower. Moreover, the ³MLCT state would be vibrationally hot, accommodating 6000–7000 cm^{-1} of energy per molecule released during intersystem crossing from the optically populated singlet state.

The instantaneous shift is attributed to the redistribution of electron density upon excitation of the rhenium chromophore at the ground-state geometry of both the chromophore and its environment. Orientation of solvent and protein dipoles would be fixed in response to the ground-state chromophore polarity, exerting an electric field that would limit the extent of charge transfer from Re^I(CO)₃ to the phen ligand, which in turn would diminish the magnitude of the instantaneous shift relative to the overall shift seen for the relaxed state. The magnitude of the instantaneous shift would be diminished further by anharmonic coupling between A'(1) $\nu(\text{CO})$ and low-frequency, large-amplitude vibrations, which would be initially highly excited. The instantaneous shift was found to be larger for the Re^I–azurins (14–18 cm^{-1}) than for [Re^I(CO)₃(phen)(im)]⁺ (9 cm^{-1}). Moreover, the effect is greater for Re^I(CO)₃(phen)(His83)Az [where the metallolabel is surrounded on two sides by different regions of the protein and is in close proximity to several negatively charged residues (Figure 4)] than for Re^I(CO)₃(phen)(His109)Az, where the complex contacts the polypeptide only in the region surrounding the coordinating histidine (Figure 5).

(40) Glyn, P.; George, M. W.; Hodges, P. M.; Turner, J. J. *J. Chem. Soc., Chem. Commun.* **1989**, 1655–1657.

(41) Breidenbeck, J.; Helbing, J.; Hamm, P. *J. Am. Chem. Soc.* **2004**, *126*, 990–991.

(42) Connick, W. B.; Di Bilio, A. J.; Hill, M. G.; Winkler, J. R.; Gray, H. B. *Inorg. Chim. Acta* **1995**, *240*, 169–173.

(43) Because of uncertainties in band-shape fitting, this analysis can only be semiquantitative, although the parameters summarized in Table 2 allow reliable comparisons to be made among individual compounds.

We suggest that the increase in the instantaneous shift on going from $[\text{Re}^{\text{I}}(\text{CO})_3(\text{phen})(\text{im})]^+$ in D_2O to the Re^{I} -azurins is caused by the lower polarity near the protein surface along with smaller exposure of the rhenium chromophore to the solvent, which allow for larger electron density redistributions upon excitation. The vibrational contribution to the instantaneous shift is mainly an intramolecular effect, assumed to be comparable for the Re^{I} -azurins and $[\text{Re}^{\text{I}}(\text{CO})_3(\text{phen})(\text{im})]^+$.

The fast component of the dynamic shift contains contributions from vibrational cooling of the excited-state chromophore (e.g., dissipation of energy from low-frequency vibrations into the solvent) and fast reorientation of D_2O molecules in the solvation. A similar fast component has been observed for Re^{I} -tricarbonyl complexes in aprotic solvents (CH_3CN , DMF, CH_2Cl_2) as well as alcohols and even at a bare ZrO_2 surface.^{20,25,39,44–46} The fast component is the dominant contribution, accounting for 80–70% of the dynamic shift. The time constants measured for the Re^{I} -azurins (~ 4 ps) are longer than that of $[\text{Re}^{\text{I}}(\text{CO})_3(\text{phen})(\text{im})]^+$ in D_2O (2.1 ps). This difference probably reflects a slower reorientation of D_2O molecules in the protein vicinity as compared to the bulk solvent and a slower rate of vibrational energy transfer⁴⁷ from the rhenium chromophore to the protein.

The slow component of the dynamic shift reports on the structural response of the rhenium chromophore environment and surface-bound D_2O to the change of the charge distribution within the chromophore upon MLCT excitation. While its magnitudes are rather small (18–27% of the dynamic shift) and comparable for both Re^{I} -azurins and $[\text{Re}^{\text{I}}(\text{CO})_3(\text{phen})(\text{im})]^+$, the dynamics are vastly different. The rate of the “slow” dynamic shift component for the Re^{I} -azurins is at least 20-times slower than that for $[\text{Re}^{\text{I}}(\text{CO})_3(\text{phen})(\text{im})]^+$ (~ 250 and 9.5 ps). This effect is related to the rate of structural adjustment near the rhenium chromophore caused by charge redistribution, that is, to flexibility in the region of the metallolabel. The environmental response includes several contributions, among them the reorientation of D_2O molecules, which is slower if the water is bound to a protein surface than in the bulk.^{48–51} However, the rates of the “slow” kinetics component determined

for Re^{I} -azurins are much slower than those of surface–water relaxation found for other proteins (30–60 ps).^{48–51} Because the reorientation time of D_2O is expected^{52,53} to be similar to that of H_2O , we conclude that the “slow” dynamics of the rhenium chromophore does not originate solely in the reorientation of surface D_2O molecules, which is 4–5 times faster.⁴⁹

The protein-bound rhenium complex is solvated much less than $[\text{Re}^{\text{I}}(\text{CO})_3(\text{phen})(\text{im})]^+$ (Figures 4 and 5). Reorientation of the rhenium chromophore relative to nearby polar amino acid residues as well as polypeptide dynamics are important contributors to the relaxation process. These motions likely are the main contributors to slowing medium reorganization in Re^{I} -azurins, relative to both the bulk and the protein-bound water.^{48–51} Rotational freedom of the rhenium unit about the $\text{His } C^\alpha\text{--}C^\beta$ bond is demonstrated by the two conformations of the rhenium complex in $\text{Re}^{\text{I}}(\text{CO})_3(\text{phen})(\text{His}109)\text{Az}$ (Figure 5). $\text{Re}^{\text{I}}(\text{CO})_3(\text{phen})(\text{His}109)\text{Az}$, whose structure in the region of the rhenium complex is much more flexible than that of $\text{Re}^{\text{I}}(\text{CO})_3(\text{phen})(\text{His}83)\text{Az}$, exhibits a faster relaxation rate.

In conclusion, although the ³MLCT excited states of $\text{Re}^{\text{I}}(\text{CO})_3(\text{phen})(\text{His}X)\text{Az}$ ($X = 83, 109$) and $[\text{Re}^{\text{I}}(\text{CO})_3(\text{phen})(\text{im})]^+$ after full relaxation (thermal equilibration) of the rhenium chromophore and its environment are virtually the same, the relaxation mechanism and dynamics are very different. Bulk D_2O allows for less charge separation immediately after excitation than the lower dielectric region near the rhenium unit. However, there is larger-scale medium (outer-sphere) dynamic reorganization of bulk D_2O than for the proteins. The much slower relaxation rate seen for both Re^{I} -azurins, as compared to $[\text{Re}^{\text{I}}(\text{CO})_3(\text{phen})(\text{im})]^+$ in bulk D_2O , is attributed mainly to structural changes associated with reorientation of protein-bound D_2O molecules and nearby restrained protein dipoles. We conclude that protein-bound Re^{I} -carbonyl–polypyridyl complexes can function as sensitive reporters of the dynamic responses of surface D_2O molecules as well as the polypeptide in the region around the rhenium unit.

Acknowledgment. This work was supported by the NIH (DK19038), NSF (MCB: 0133564), EPSRC, CCLRC, and QMUL.

JA057451+

- (44) Lenchenkov, V. A.; She, C. X.; Lian, T. Q. *J. Phys. Chem. B* **2004**, *108*, 16194–16200.
(45) Busby, M.; Matousek, P.; Towrie, M.; Clark, I. P.; Motevalli, M.; Hartl, F.; Vlček, A. *Inorg. Chem.* **2004**, *43*, 4523–4530.
(46) Bredenbeck, J.; Helbing, J.; Hamm, P. *Phys. Rev. Lett.* **2005**, *95*.
(47) Yu, X.; Leitner, D. M. *J. Phys. Chem. B* **2003**, *107*, 1698–1707.
(48) Pal, S. K.; Peon, J.; Zewail, A. H. *Proc. Natl. Acad. Sci. U.S.A.* **2002**, *99*, 1763–1768.
(49) Pal, S. K.; Zewail, A. H. *Chem. Rev.* **2004**, *104*, 2099–2123.
(50) Kamal, J. K. A.; Zhao, L.; Zewail, A. H. *Proc. Natl. Acad. Sci. U.S.A.* **2004**, *101*, 13411–13416.

- (51) Bhattacharyya, S. M.; Wang, Z. G.; Zewail, A. H. *J. Phys. Chem. B* **2003**, *107*, 13218–13228.
(52) Shirota, H.; Pal, H.; Tominaga, K.; Yoshihara, K. *J. Phys. Chem.* **1996**, *100*, 14575–14577.
(53) Tominaga, K.; Klinier, D. A. V.; Johnson, A. E.; Levinger, N. E.; Barbara, P. F. *J. Chem. Phys.* **1993**, *98*, 1228–1243.